26. J. P. Cleveland, S. Manne, D. Bocek, P. K. Hansma, *Rev. Sci. Instrum.* **64**, 403 (1993).
27. W. A. Ducker, T. J. Senden, R. M. Pashley, *Langmuir* **8**, 1831 (1992).
28. D. K. Newman, R. Kolter, *Nature* **405**, 94 (2000).
29. T. J. DiChristina, E. F. Delong, *J. Bacteriol.* **176**, 1468 (1994).
30. A. S. Beliaev, D. A. Saffarini, *J. Bacteriol.* **180**, 6292 (1998).
31. I. Sokolov, D. S. Smith, G. S. Henderson, Y. A. Gorby, F. G. Ferris, *Environ. Sci. Tech.* **35**, 341 (2001).
32. W. Stumm, J. J. Morgan, *Aquatic Chemistry: Chemical Equilibria and Rates in Natural Waters* (Wiley, New York, ed. 3, 1996), pp 534–540.
33. S. Brown, *Proc. Natl. Acad. Sci. U.S.A.* **89**, 8651 (1992).
34. N. Ohmura, K. Kitamura, H. Saiki, *Appl. Environ. Microbiol.* **59**, 4044 (1993).
35. T. J. Beveridge, *J. Bacteriol.* **181**, 4725 (1999).
36. On the basis of transmission electron microscopy and freeze-substitution analyses, extracellular polysaccharide, a common macromolcule on the surface of many bacteria, has not been detected on the cell wall of *S. oneidensis* (A. Korenevsky and T. Beveridge, unpublished data).
37. P. J. Flory, *Statistical Mechanics of Chain Molecules* (Hanser, New York, 1989), pp. 401–403.
38. M. Rief, M. Gautel, F. Oesterhelt, J. M. Fernandez, H. E. Gaub, *Science* **276**, 1109 (1997).
39. H. Mueller, H.-J. Butt, E. Bamberg, *Biophys. J.* **76**, 1072 (1999).
40. D. J. Muller, W. Baumeister, A. Engel, *Proc. Natl. Acad. Sci. U.S.A.* **96**, 13170 (1999).
41. J.-J. Karlsson, A. Kadziola, A. Rasmussen, T. E. Rostrup, J. Ulstrup, in *Protein Folds: A Distance-Based Approach*, H. Bohr, S. Brunak, Eds. (CRC Press, Boca Raton, FL, 1996), pp. 56–67.
42. J. M. Myers, C. R. Myers, *Appl. Environ. Microbiol.* **67**, 260 (2001).
43. Future studies will use biological force microscopy with mutants incapable of producing and/or secreting cell wall biomolecules such as the 150-kD protein.
44. G. V. Bloemberg, G. A. O'Toole, B. J. J. Lugtenberg, R. Kolter, *Appl. Environ. Microbiol.* **63**, 4543 (1997).
45. N. P. D'Costa, J. H. Hoh, *Rev. Sci. Instrum.* **66**, 5096 (1995).

46. We thank B. Lower, C. Myers, J. Banfield, and the anonymous reviewers for constructive comments; G. O'Toole for providing plasmid pSMC2; and J. Tak for support. This manuscript is dedicated to B. Diehl. Mineral samples were provided by the Virginia Tech Geological Sciences Museum. Financial support was provided by the U.S. Department of Energy and the NSF.

5 February 2001; accepted 4 April 2001

Ultrafast Source-to-Surface Movement of Melt at Island Arcs from ^{226}Ra-^{230}Th Systematics

Simon Turner,[1,2]* Peter Evans,[1,3] Chris Hawkesworth[1,2]

Island arc lavas have radium-226 excesses that extend to higher values than those observed in mid-ocean ridge or ocean island basalts. The initial ratio of radium-226 to thorium-230 is largest in the most primitive lavas, which also have the highest barium/thorium ratios, and decreases with increasing magmatic differentiation. Therefore, the radium-226 excesses appear to have been introduced into the base of the mantle melting column by fluids released from the subducting plate. Preservation of this signal requires transport to the surface arguably in only a few hundreds of years and directly constrains the average melt velocity to the order of 1000 meters per year. Thus, melt segregation and channel formation can occur rapidly in the mantle.

The velocity of melt ascent from its source through Earth's mantle and crust to the surface is extremely hard to determine, even though such measurements would place important constraints on the mechanisms of melt transport and the physical behavior of the mantle during partial melting (*1–5*). Disequilibria between the short-lived U-series isotopes can provide estimates of melt velocities and have recently been used to show that mantle melt velocities are too fast for transport to occur by grain-scale percolation mechanisms all the way to the surface. Instead, melt must, at some critical stage, separate into discrete channels (*1–5*). What remains to be determined is how quickly melt moves and at what melt fraction such channels form. The short-lived U-series isotope ^{226}Ra has a half-life of only 1600 years and can be used to estimate melt velocity and residual porosity (*1–5*). However, recent models for melt formation and transport beneath mid-ocean ridges and ocean islands emphasize that ^{226}Ra-^{230}Th disequilibria is created throughout the melting column and the disequilibria measured at the surface only reflects that produced in the upper portions of the melting column (*3–5*). Thus, although ^{226}Ra disequilibria in mid-ocean ridge and ocean island basalts (MORB and OIB, respectively) provide important constraints on the residual porosity, they do not place tight constraints on the melt velocity because the depth of origin of the disequilibria is debatable.

No global ^{226}Ra study has been conducted on island arc lavas since the pioneering investigation of Gill and Williams (*6*), who suggested that ^{226}Ra excesses might be related to fluid addition. Accordingly, we have undertaken high-precision, mass spectrometric measurements of ^{226}Ra disequilibria in 40 historic lavas from seven island arcs that, combined with recent data from the Tonga-Kermadec arc (*7*), allow us to evaluate the global ^{226}Ra-^{230}Th systematics in island arc rocks. The $(^{226}Ra/^{230}Th)_o$ values (where the parentheses denote activity ratios) extend to ^{226}Ra excesses of over 600% and show a significant variation above each arc (Table 1), ranging from 0.87 to 2.66 in the Lesser Antilles, 1.25 to 4.96 in Vanuatu, 1.51 to 1.59 in the Philippines (two samples only), 1.06 to 5.44 in the Marianas, 1.39 to 4.16 in the Aleutians, 1.00 to 3.53 in Kamchatka, 0.94 to 3.71 in Indonesia, and 0.93 to 6.13 in Tonga-Kermadec (*7*). Only one sample has $(^{226}Ra/^{230}Th)_o < 1$, and five samples are within analytical error of 1.

The $(^{226}Ra/^{230}Th)_o$ versus $(^{238}U/^{230}Th)$ diagram (Fig. 1) illustrates that the U-series disequilibria in island arc lavas are distinct from MORB and OIB, extending to higher $(^{226}Ra/^{230}Th)_o$ ratios and having the reverse sense of U-Th fractionation. Thus, the island arc lavas with the highest $(^{226}Ra/^{230}Th)_o$ are crudely correlated with the highest $(^{238}U/^{230}Th)$ (*8–11*). Some aspects of these different tectonic regimes are similar, in that melting is initiated at depths of 100 km and the total extent of melting is probably in the range 8 to 15%. However, for MORB and OIB, melting occurs in response to decompression. The ^{230}Th excesses [i.e., $(^{238}U/^{230}Th) < 1$] reflect the greater compatibility of U, relative to Th in residual aluminous clinopyroxene and garnet (*12*, *13*) and have been used to constrain the mantle upwelling and melting rates in these regions (*1–5*). The porosities required to obtain $(^{226}Ra/^{230}Th)_o > 3$ by decompression melting alone are <0.0001% (*1–5*) and most MORB and OIB have $(^{226}Ra/^{230}Th)_o < 3$ (Fig. 1) (*14–22*). In contrast, melting beneath island arcs is linked to the lowering of the peridotite solidus by addition of aqueous fluids released during dehydration reactions in the downgoing plate (*23*, *24*), and the role of decompression on melting has proved hard to resolve (*25–27*). The ^{238}U excesses that typify

[1]Department of Earth Sciences, The Open University, Walton Hall, Milton Keynes MK7 6AA, UK. [2]Department of Earth Sciences, Wills Memorial Building, University of Bristol, Bristol BS8 1RJ, UK. [3]Laboratories of the Government Geochemist, Queens Road, Teddington, Middlesex PW11 0LY, UK.

*To whom correspondence should be addressed. E-mail: simon.turner@bristol.ac.uk

island arc lavas (Fig. 1) are inferred to reflect U addition by the aqueous fluids (*8–10*, *27–43*), and correlations between ($^{230}Th/^{232}Th$) and ($^{238}U/^{232}Th$) have been used to suggest that this typically occurs 20,000 to 150,000 years before eruption (*8–10*, *27–43*). The ^{226}Ra-^{230}Th and ^{238}U-^{230}Th disequilibria in island arc lavas are, therefore, different from those in MORB and OIB, and they cannot be accounted for by partial melting processes in the same way because that should result in ^{230}Th excesses and ^{226}Ra excesses ≤ 3 (*44*).

A $(^{226}Ra/^{230}Th)_o$ versus SiO_2 diagram (Fig. 2) shows that the highest Ra-Th disequilibria occur in the least differentiated lavas, some of which represent near primary melts. These lavas also have the lowest $^{87}Sr/^{86}Sr$, and no common assimilant with Ra and Ba $\gg$ Th has yet been identified. This emphasizes that the ^{226}Ra excesses in island arc magmas are a mantle feature and were not superimposed on the magmas at shallow levels through interaction with seawater, hydrothermal fluids, or crustal materials. The ^{226}Ra excesses $(^{226}Ra/^{230}Th)_o$ decrease with increasing differentiation, as has been observed in other tectonic settings (*45*, *46*). This is unlikely to be due to Ra/Th fractionation by crystal-liquid differentiation because Ra and Th remain incompatible elements while the liquidus assemblage is gabbroic (Fig. 2), although evolved liquids may undergo decreases in Ra/Th as the proportion of plagioclase in the crystallizing assemblages increases (*47*). If the decreases in $(^{226}Ra/^{230}Th)_o$ reflect the time taken for crystal-liquid differentiation (*48*), then the rate of decrease in $(^{226}Ra/^{230}Th)_o$ can be used to calibrate the time scale for differentiation [e.g. (*7*, *46*)]

Table 1. ^{226}Ra disequilibria for subduction zone lavas with references for sample information and supporting geochemical and isotopic data including ($^{238}U/^{230}Th$) ratios. Repeat analyses of the Mt. Lassen rock standard (*59*) yielded $^{226}Ra = 1065 \pm 9$ fg/g ($n = 6$), and the reproducibility of ($^{226}Ra/^{230}Th$) is estimated to be 1.3% (2σ). Measured ^{226}Ra concentrations (denoted by subscript m) were age corrected to initial activities and activity ratios (denoted by subscript o), assuming the decay constant $\lambda^{226}Ra = 4.332 \times 10^{-4}$. (The data from the St. Kitts lavas, Lesser Antilles, must be treated with caution due to the magnitude of the required age correction.) Further details of the chemical separation and mass spectrometry techniques used are given in (*7*).

Sample no.	Island or volcano	Eruption age (A.D.)	SiO_2 (wt. %)	Ba (ppm)	Th (ppm)	$^{226}Ra_m$ (fg/g)	$(^{226}Ra)_o$ (Bq)	$(^{226}Ra/^{230}Th)_o$	Reference
				Lesser Antilles					
Kit45b	St. Kitts	0280	56.1	124	0.602	84.84	0.000151	0.873	(*28–32*)
Kit50	St. Kitts	0200	51.8	130	0.687	124.12	0.000286	1.458	(*28–32*)
MVO244	Montserrat	1998	60.2	247	2.447	263.25	0.000505	0.992	(*28–32*)
MVO372	Montserrat	1998	-	-	3.011	311.25	0.000597	1.020	(*28–32*)
M8222	Martinique	1792	59.1	202	2.478	239.44	0.000459	1.003	(*28–32*)
M8225	Martinique	1929	60.3	224	2.225	245.94	0.000473	1.161	(*28–32*)
STV354	St. Vincent	1979	52.9	133	1.052	325.21	0.000627	2.214	(*28–32*)
STV371	St. Vincent	1590	54.8	110	0.851	299.50	0.000636	2.655	(*28–32*)
RW 33	Ile de Caille	1000	47.9	106	2.051	245.34	0.000481	1.069	(*28–32*)
K I	Kick 'em Jenny	1974	51.2	178	2.901	723.66	0.001388	1.397	(*28–32*)
				Vanuatu					
Lopevi bomb	Lopevi	1970	50.4	128	0.561	381.91	0.000738	4.959	(*33*)
Yasur 1975	Tanna	1975	54.9	512	2.376	485.16	0.000931	1.250	(*33*)
Yasur 1993	Tanna	1993	56.0	552	2.226	608.97	0.001167	1.659	(*33*)
68553	Matthew	1940	62.0	138	1.620	392.04	0.000759	1.672	(*33*)
68557	Matthew	1940	63.2	159	1.314	271.58	0.000524	1.415	(*33*)
				Philippines					
1968	Mt. Mayon	1968	54.7	353	1.768	306.06	0.000589	1.512	(*34*, *35*)
1984	Mt. Mayon	1984	54.7	363	2.033	316.75	0.000608	1.589	(*34*, *35*)
				Mariana					
PA1	Pagan	1981	51.5	225	0.620	218.96	0.000421	2.772	(*36*, *37*)
GU6	Guguan	1883	52.0	164	0.360	196.41	0.000390	4.227	(*36*, *37*)
GU9	Guguan	1883	50.9	163	0.324	223.85	0.000447	5.442	(*36*, *37*)
U4	Uracas	1952	57.9	317	0.960	134.87	0.000260	1.145	(*36*, *37*)
U2	Uracas	1952	58.8	351	1.110	144.25	0.000277	1.061	(*36*, *37*)
				Aleutians					
UM21	Umnak	1946	52.2	239	1.174	229.62	0.000442	1.359	(*38*)
KAN 5-8	Kanaga	1900	53.7	552	3.497	671.97	0.001302	1.389	(*38*)
K81-7A	Kasatochi	1899	49.1	227	1.078	335.73	0.000669	2.234	(*38*)
BOG 1796	Bogoslof	1796	61.0	1839	4.814	2727.32	0.005572	4.155	(*38*)
				Kamchatka					
TB-9-7-75	Tolbachik	1975	49.7	263	0.527	389.64	0.000753	3.529	(*38*)
T889	Tolbachik	1976	50.4	357	1.134	392.13	0.000754	1.704	(*38*)
A4-91	Avachinsky	1991	55.9	301	0.639	189.81	0.000365	2.097	(*38*)
G574	Gorely	1390	52.3	337	0.873	128.65	0.000246	0.997	(*38*)
2562	Sheveluch	1964	58.2	442	1.228	435.37	0.000841	2.024	(*38*)
J4497	Karymsky	1976	62.4	409	1.692	403.80	0.000776	1.248	(*38*)
J4499	Karymsky	1971	62.2	401	1.603	392.88	0.000755	1.250	(*38*)
				Sunda					
L2835	Krakatau	1883	57.9	321	7.453	701.85	0.001286	0.983	(*39*)
VB82	Galunggung	1982	49.1	48	0.777	107.80	0.000207	2.000	(*39*)
M15	Merapi	1006	52.0	405	4.890	408.03	0.000832	1.209	(*39*)
LBK/86/1	Rindjani	1900	53.6	430	4.251	506.86	0.000981	1.345	(*39*)
T205/88	Tambora	1815	55.5	1201	11.857	1278.99	0.002482	1.203	(*39*)
SA88/303	Sangeang Api	1985	51.7	1578	10.180	2119.27	0.004070	2.467	(*39*)
FL26	Iya	1900	51.8	92	0.439	114.33	0.000226	3.714	(*39*)

which must be less than the 8000-year period required for $(^{226}Ra/^{230}Th)_o$ to return to unity. Alternatively, if such decreases in $(^{226}Ra/^{230}Th)_o$ are due to mixing processes, as indicated when $(^{238}U/^{230}Th)$ also decreases with increasing SiO_2 despite the longer half-life (*49*), or instead reflect evolution from lower $(^{226}Ra/^{230}Th)_o$ parents, any time estimates would be a maximum and differentiation might be almost instantaneous. Thus, if melts do stall in the crust it is generally for short periods of time (<8000 years) and it appears that the majority of island arc basalts and andesites spend less than a few thousand years traversing the crust (*6*, *9*, *40*).

The most striking observation is that there is a broad correlation between $(^{226}Ra/^{230}Th)_o$ and Ba/Th ratio (Fig. 3), both globally and within almost every island arc (*7*, *9–11*). Radium-226 enrichments in MORB and OIB are typically smaller (*14–22*) and occur without accompanying increases in Ba. In island arc lavas, Ba/Th is widely regarded as a diagnostic ratio for identifying the fluid component added from the subducting plate (*7–10*, *27–43*). These correlations, combined with the inability of partial melting processes to explain the coupled ^{226}Ra-^{230}Th and ^{238}U-^{230}Th disequilibria (see melting curves in Fig. 1), suggest that the addition of aqueous fluids was responsible for the ^{226}Ra-^{230}Th disequilibria observed in island arc lavas (*6*, *7*). This implies much faster transfer times for the fluid component, perhaps by hydrofracture (*50*), than estimates of 20,000 to 150,000 years based on U-Th disequilibria (*8–10*, *27–43*). One explanation is that those interpretations were in error and that U was also added to the wedge very recently (*11*). However, in the Tonga-Kermadec arc, time scales derived from both the U-Th and U-Pa systems are in close agreement (*27*, *42*, *43*). An alternative interpretation is that U and Ra were added by fluids that were spatially and temporally separated (*7*), consistent with a general notion that addition of subducted components to island arc sources is a multi-stage process (*7–10*, *27–43*). Either way, an inescapable conclusion is that the ^{226}Ra excesses were produced less than 8000 years ago. In practice, it is probable that they were produced much more recently because, if even a single half-life (1600 years) has elapsed, the primary ^{226}Ra excesses would have had to have been twice as large (up to 1200%). It is probable, therefore, that only a few hundreds of years have elapsed since the generation of the ^{226}Ra excesses.

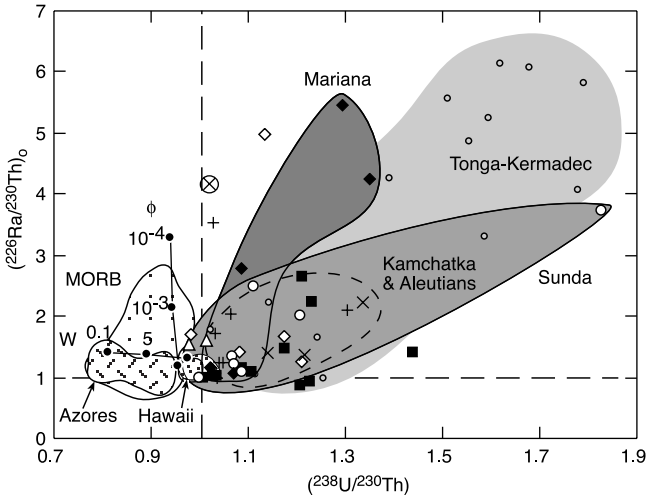

Fig. 1. Plot of $(^{226}Ra/^{230}Th)_o$ versus $(^{238}U/^{230}Th)$ contrasting the new data from island arc lavas with data from mid-ocean ridges (*14–19*) and selected ocean islands (*20–22*, *56*) (Hawaiian field plots tholeiites only). The dynamic melting curves (*57*) illustrate that, for ridges and ocean islands, $(^{226}Ra/^{230}Th)_o$ is largely a function of residual porosity (ϕ), which varies from 0.01% near the equipoint to 0.001% and 0.0001%, whereas $(^{238}U/^{230}Th)$ is primarily controlled by upwelling rate (W) which varies from 10 cm·yr^{-1} near the equipoint to 5 cm·year^{-1} and 0.1 cm·year^{-1}. In contrast, lavas from island arcs are characterized by $(^{238}U/^{230}Th) > 1$ and high $(^{226}Ra/^{230}Th)_o$ ratios which are broadly correlated and cannot be produced by dynamic melting models (*44*). Tonga-Kermadec data here and in Figs. 2 and 3 are from (*7*, *43*). Lesser Antilles (■), Kamchatka (+), Mariana (◆), Vanuatu (◇), Sunda (○), Philippines (△), Aleutians (×), and Bogoslof (⊗), which is located north of the Aleutian arc front. Dashed horizontal and vertical lines indicate secular equilibrium.

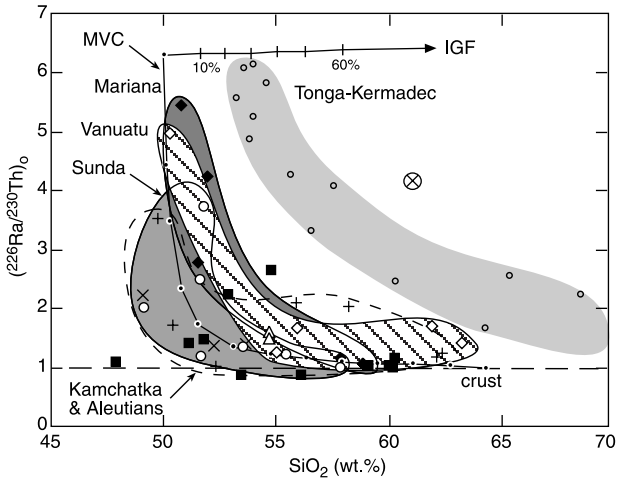

Fig. 2. Plot of $(^{226}Ra/^{230}Th)_o$ versus SiO_2 showing that the largest $(^{226}Ra/^{230}Th)_o$ ratios are found in the most primitive lavas, indicating a mantle origin for this disequilibria. $(^{226}Ra/^{230}Th)_o$ decreases with increasing SiO_2, which places constraints on the time scale of differentiation. A model, instantaneous gabbroic fractionation vector (IGF) (*58*), shows that Ra/Th remains essentially constant during fractionation from basalt to dacite. If the observed decrease in $(^{226}Ra/^{230}Th)_o$ is due to the time taken for crystal-liquid differentiation, then this must have taken less than the 8000 years. Alternatively, the $(^{226}Ra/^{230}Th)_o$ versus SiO_2 arrays might reflect mixing between high $(^{226}Ra/^{230}Th)$ mafic melts and felsic crustal melts (curve labeled MVC) in ^{226}Ra-^{230}Th equilibrium as illustrated by the model mixing curve (*58*) shown (10% crustal addition increments indicated). Symbols are as in Fig. 1; dashed horizontal line indicates secular equilibrium.

Another key point is that the individual arrays on Fig. 3 extend to $(^{226}Ra/^{230}Th)_o = 1$ at variable Ba/Th ratios, which may mean those Ba/Th variations were developed during fluid addition that occurred long enough ago for $(^{226}Ra/^{230}Th)_o$ to have returned to secular equilibrium (i.e., >8000 years ago). More important, because melting models predict that all zero-age MORB and OIB are likely to have some ^{226}Ra excess (*1–5*), the island arc arrays would be expected to terminate at $(^{226}Ra/^{230}Th)_o > 1$ (Fig. 3) if there were a ubiquitous decompression melting effect on ^{226}Ra-^{230}Th disequilibria beneath island arcs (*51*).

The ^{226}Ra excesses in island arc lavas appear to have been introduced into their mantle source by fluids. If these fluids are the catalyst for partial melting, they define the base of the melting column and provide a direct constraint on the total melt transit time, which has to be shorter than the half-life of ^{226}Ra. For total transit times of ~100 years, the required source-to-surface melt velocity is ~1000 m·year^{-1}, and this ignores any time taken for fluid transfer from the subducting plate to the melting column. Moreover, because the calculation also includes time spent in the crust (Fig. 2), the implied velocities through the mantle may be even faster. The estimated velocities require channeled flow rather than grain scale percolation (*1–5*, *52*, *53*) and so transient, millimeter-sized veins must form rapidly and deep in the source region. The required melt velocities also limit the amount of melt–wall rock equilibration that

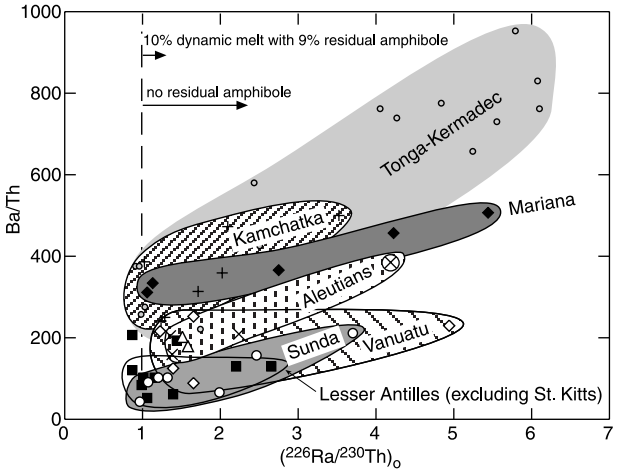

Fig. 3. Plot of Ba/Th versus $(^{226}Ra/^{230}Th)_o$ showing that the largest $(^{226}Ra/^{230}Th)_o$ ratios occur in those lavas that have the highest Ba/Th ratios and that, in general, there is a positive correlation between these indices. Ba/Th ratios provide a sensitive monitor of the effects of fluid addition (*7–10*, *27–43*) and the correlations suggest that this is the origin of the ^{226}Ra excesses in island arc lavas. Melting vectors show the magnitude of $(^{226}Ra/^{230}Th)_o$ disequilibria expected from partial melting processes (*51*), yet the island arc lava arrays extend to $(^{226}Ra/^{230}Th)_o = 1$. Symbols are as in Fig. 1; dashed vertical line indicates secular equilibrium.

can take place to create negative niobium anomalies (*54*) or other U-series disequilibria (*4*, *5*). For example, the development of ^{231}Pa excesses in island arc lavas (*27*, *55*) by equilibrium porous flow (*4*, *5*) would require a residual porosity $<0.0001\%$ if the small inferred distribution coefficient of Pa (*13*) is to lead to melting-induced ^{231}Pa excesses overwriting fluid-induced ^{235}U excesses (*27*, *55*), and mixing may be an alternative.

In conclusion, island arc melting models need to incorporate high melt ascent velocities. Such conditions probably reflect the vigor of fluid-induced melting compared with MORB and OIB, where melting rates are dictated by upwelling rates on the order of a few centimeters per year. However, it may be that these velocities are generally applicable, in which case the long-held notion of basalts migrating slowly through the mantle in interconnected but vanishingly small pore spaces will have to be abandoned.

References and Notes

1. D. McKenzie, *Earth Planet. Sci. Lett.* **72**, 149 (1985).
2. R. W. Williams, J. B. Gill, *Geochim. Cosmochim. Acta* **53**, 1607 (1989).
3. D. McKenzie, *Chem. Geol.* **162** 81 (2000).
4. M. Spiegelman, T. Elliott, *Earth Planet. Sci. Lett.* **118**, 1 (1993).
5. C. C. Lundstrom, J. Gill, Q. Williams, *Chem. Geol.* **162**, 105 (2000).
6. J. B. Gill, R. W. Williams, *Geochim. Cosmochim. Acta* **54**, 1427 (1990).
7. S. Turner, B. Bourdon, C. Hawkesworth, P. Evans, *Earth Planet. Sci. Lett.* **179**, 581 (2000).
8. J. B. Gill, J. D. Morris, R. W. Johnson, *Geochim. Cosmochim. Acta* **57**, 4269 (1993).
9. M. K. Reagan, J. D. Morris, E. A. Herrstrom, M. T. Murrell, *Geochim. Cosmochim. Acta* **58**, 4199 (1994).
10. J. A. Hoogewerff *et al.*, *Geochim. Cosmochim. Acta* **61**, 1057 (1997).
11. F. Chabaux, C. Hémond, C. J. Allègre, *Chem. Geol.* **153**, 171 (1999).
12. P. Beattie, *Nature* **363**, 63 (1993).
13. B. J. Wood, J. D. Blundy, J. A. C. Robinson, *Geochim. Cosmochim. Acta* **63**, 1613 (1999).
14. K. H. Rubin, J. D. Macdougall, *Nature* **335**, 158 (1988).
15. S. J. Goldstein, M. T. Murrell, D. E. Janecky, *Earth Planet. Sci. Lett.* **96**, 134 (1989).
16. ———, J. R. Delaney, D. A. Clauge, *Earth Planet. Sci. Lett.* **107**, 25 (1991).
17. A. M. Volpe, S. J. Goldstein, *Geochim. Cosmochim. Acta* **57**, 1233 (1993).
18. C. C. Lundstrom, J. Gill, Q. Williams, B. B. Hanan, *Earth Planet. Sci. Lett.* **157**, 167 (1998).
19. Note that recent data show some MORB extend to $(^{226}Ra/^{230}Th) = 4.2$ [C. C. Lundstrom, D. E. Sampson, M. R. Perfit, J. Gill, Q. Williams, *J. Geophys. Res.* **104**, 13035 (1999)].
20. A. S. Cohen, R. K. O'Nions, *Earth Planet. Sci. Lett.* **120**, 169 (1993).
21. K. W. W. Sims *et al.*, *Geochim. Cosmochim. Acta* **63**, 4119 (1999).
22. S. Turner, unpublished data.
23. A. E. Ringwood, *J. Geol. Soc. London* **130**, 183 (1974).
24. Y. Tatsumi, D. L. Hamilton, R. W. Nesbitt, *J. Volcanol. Geotherm. Res.* **29**, 293 (1986).
25. T. Plank, C. H. Langmuir, *Earth Planet. Sci. Lett.* **90**, 349 (1988).
26. J. A. Pearce, I. J. Parkinson, *Geol. Soc. London Spec. Publ.* **76**, 373 (1993).
27. B. Bourdon, S. Turner, C. Allegre, *Science* **286**, 2491 (1999).
28. S. Turner *et al.*, *Earth Planet. Sci. Lett.* **142**, 191 (1996).
29. E. Heath, S. P. Turner, R. Macdonald, C. J. Hawkesworth, P. van Calsteren, *Earth Planet. Sci. Lett.* **160**, 49 (1998).
30. E. Heath, R. Macdonald, H. Belkin, C. Hawkesworth, H. Sigurdsson, *J. Petrol.* **39**, 1721 (1998).
31. C. A. Williams, thesis, The Open University (2000).
32. G. F. Zellmer, R. S. J. Sparks, C. J. Hawkesworth, L. E. Thomas, T. S. Brewer, in preparation.
33. S. P. Turner, D. W. Peate, C. J. Hawkesworth, S. M. Eggins, A. J. Crawford, *Geology* **27**, 963 (1999).
34. C. J. Hawkesworth, S. P. Turner, F. McDermott, D. W. Peate, P. van Calsteren, *Science* **276**, 551 (1997).
35. S. Turner, unpublished data.
36. F. McDermott, C. Hawkesworth, *Earth Planet. Sci. Lett.* **104**, 1 (1991).
37. J. D. Woodhead, *Chem. Geol.* **76**, 1 (1989).
38. S. Turner, F. McDermott, C. Hawkesworth, P. Kepezhinskas, *Contrib. Mineral. Petrol.* **133**, 217 (1998).
39. S. Turner, J. Foden, *Contrib. Mineral. Petrol.*, in press.
40. O. Sigmarsson, M. Condomines, J. D. Morris, R. S. Harmon, *Nature* **346**, 163 (1990).
41. T. Elliott, T. Plank, A. Zindler, W. White, B. Bourdon, *J. Geophys. Res.* **102**, 14991 (1997).
42. S. Turner, C. Hawkesworth, *Nature* **389**, 568 (1997).
43. S. Turner *et al.*, *Geochim. Cosmochim. Acta* **61**, 4855 (1997).
44. For melting processes to produce both $(^{238}U/^{230}Th)$ and $(^{226}Ra/^{230}Th)_o > 1$ requires melting at very low residual porosity at depths shallower than 37 km, where bulk distribution coefficients $D_U < D_{Th}$ in clinopyroxene; at greater depths $D_U > D_{Th}$ in clinopyroxene (*13*). This is unlikely at island arcs where melting is probably initiated at depths of ~100 km and reaches 10 to 20%.
45. C. Claude-Ivanaj, B. Bourdon, C. J. Allègre, *Earth Planet. Sci. Lett.* **164**, 99 (1998).
46. N. Vigier, B. Bourdon, J. L. Joron, C. J. Allègre, *Earth Planet. Sci. Lett.* **174**, 81 (1999).
47. G. Zellmer, S. Turner, C. Hawkesworth, *Earth Planet. Sci. Lett.* **174**, 265 (2000).
48. The curvature of the arrays in Fig. 2 suggest that the rate of increase in SiO_2 becomes more rapid with time (possibly due to the onset of magnetite crystallization) rather than decreasing, as would be expected if crystal-liquid separation was slowed by increasing viscosity.
49. The background data sets referenced in Table 1 show that both $(^{238}U/^{230}Th)$ and $(^{226}Ra/^{230}Th)_o$ decrease with increasing SiO_2 in the Lesser Antilles and Indonesia, suggesting an important role for mixing in those island arcs. With the exception of Martinique in the Lesser Antilles [J. P. Davidson, *J. Geophys. Res.* **91**, 5943 (1986)], these increases are not strongly correlated with long-lived radiogenic isotope tracers of Sr or Nd, further suggesting that the assimilant is often preexisting, unradiogenic arc crust.
50. J. H. Davies, *Nature* **398**, 142 (1999).
51. Melting vectors assume 10% dynamic melting (*2*) with residual porosity of 0.001% and upwelling rate of 5 cm·year^{-1}. Vector with 9% residual amphibole used bulk distribution coefficients $D_U = 5.7 \times 10^{-3}$, $D_{Th} = 3.8 \times 10^{-3}$ and $D_{Ra} = 3.1 \times 10^{-3}$.
52. C. Richardson, D. McKenzie, *Earth Planet. Sci. Lett.* **128**, 425 (1994).
53. M. Spiegleman, D. McKenzie, *Earth Planet. Sci. Lett.* **83**, 137 (1987).
54. P. B. Kelemen, N. Shimizu, T. Dunn, *Earth Planet. Sci. Lett.* **120**, 111 (1993).
55. D. A. Pickett, M. T. Murrell, *Earth Planet. Sci. Lett.* **148**, 259 (1997).
56. S. Turner, C. Hawkesworth, N. Rogers, P. King, *Chem. Geol.* **139**, 145 (1997).
57. Dynamic melting vectors were derived with the model of (*2*), using bulk distribution coefficients $D_U = 3.3 \times 10^{-3}$, $D_{Th} = 1.9 \times 10^{-3}$ and $D_{Ra} = 1.8 \times 10^{-4}$.
58. Fractionation and mixing models assumed a mafic parental magma with 50% SiO_2 and $(^{226}Ra/^{230}Th)_o = 6.5$ containing 0.1 parts per million (ppm) Th. Rayleigh fractionation involved a gabbroic assemblage consisting of 21% clinopyroxene, 40% plagioclase, 27% amphibole and 12% magnetite. Distribution coefficients were as follows: clinopyroxene, $D_{Ra} = 1.7 \times 10^{-6}$ and $D_{Th} = 1.3 \times 10^{-2}$; plagioclase $D_{Ra} = 3.3 \times 10^{-2}$ and $D_{Th} = 1.0 \times 10^{-9}$; amphibole $D_{Ra} = 9.5 \times 10^{-7}$ and $D_{Th} = 2.0 \times 10^{-2}$; magnetite $D_{Ra} = 1.0 \times 10^{-9}$ and $D_{Th} = 1.0 \times 10^{-9}$. SiO_2 was calculated by least-squares mixing. The crustal contaminant had 66% SiO_2 and $(^{226}Ra/^{230}Th) = 1$ containing 10.7 ppm Th.
59. A. M. Volpe, J. A. Olivares, M. T. Murrell, *Anal. Chem.* **63**, 913 (1991).

60. Our work on island arc lavas has only been possible through the generosity of the following people whom we thank for either directly or indirectly supplying samples—S. Acland, I. Bahar, S. Bronto, T. Crawford, J. Davidson, M. Defant, S. Eggins, T. Ewart, J. Foden, J. Gamble, J. Gill, B. Kay, P. Kepezhinskas, R. Macdonald, J. Morris, J. Pearce, T. Reay, I. Smith, L. Sutherland, T. Vallier, S. Weaver, C. Williams, J. Woodhead, and T. Worthington. B. Bourdon, T. Elliott, M. Spiegleman, M. Hirschmann, and R. George are all thanked for many helpful discussions. Two anonymous reviewers are thanked for their enthusiastic and helpful comments. S.T. is funded by a Royal Society Research Fellowship and P.E. by a NERC grant (GR8/03725) to S.T.

15 February 2001; accepted 29 March 2001